PHILOSOPHICAL TRANSACTIONS OF THE ROYAL SOCIETY A MATHEMATICAL, PHYSICAL & ENGINEERING SCIENCES

Low-Frequency Seismology and the Three-Dimensional Structure of the Earth

T. G. Masters

Phil. Trans. R. Soc. Lond. A 1989 **328**, 329-349
doi: 10.1098/rsta.1989.0039

Phil. Trans. R. Soc. Lond. A **328**, 329–349 (1989)
Printed in Great Britain

Low-frequency seismology and the three-dimensional structure of the Earth

By T. G. Masters

Institute of Geophysics and Planetary Physics, University of California, San Diego, A-025, La Jolla, California 92093, *U.S.A.*

We attempt to catalogue those features of the three-dimensional structure of the Earth that are well-constrained by low-frequency data (i.e. periods longer than about 125 seconds). The dominant signals in such data are the surface-wave equivalent modes whose phase characteristics are mainly affected by a large scale structure of harmonic degree two in the upper mantle. Available aspherical models predict this phase behaviour quite well, but do not give an accurate prediction of the observed waveforms and we must appeal to higher-order structure and/or coupling effects to give the observed complexity of the data. Strong splitting of modes which sample the cores of the Earth is also observed and, though we do not yet have a model of aspherical structure which gives quantitative agreement with these data, anisotropy or large-scale aspherical structure in the inner core appears to be required to model the observed signal.

Introduction

The last few years have seen some major advances in our understanding of the large-scale aspherical structure of the Earth and it is the intention of this paper to summarize the contributions of low-frequency seismology. There are several advantages to working with low-frequency data. These are the only seismic data that are at all sensitive to the density structure of the Earth (though it will be some time before aspherical density structure is reliably determined). Furthermore, relatively simple representations of the source suffice to model the excitation of long period waves and we can be reasonably sure (for all but the largest earthquakes) that any anomalous signal we see is due to structure. Finally, attenuation appears to be only weakly frequency dependent in the free oscillation frequency band, so simplifying the modelling process. On the other hand, there are some disadvantages associated with long-period data. Perhaps the most severe of these is the low sensitivity to structure of odd harmonic degree. As we shall see, the features in the data which constrain the odd-order structure are quite subtle and we must be careful that any theoretical approximations that we make do not swamp this signal with spurious signal-generated noise. An obviously desirable way to proceed is to use both low-frequency data and shorter-period body wave data to constrain structure in a simultaneous inversion and this will undoubtedly become common in the near future.

In low-frequency seismology, it is convenient to specify structure by expansion in spherical harmonics and several models of aspherical structure incorporating structure up to harmonic degree eight or higher now exist. An alternative representation of structure calls for an *a priori* division of the surface of the sphere into various regions which are supposed to have similar seismic properties. Such *tectonic regionalizations* are, of course, subject to the prejudice of the

individual investigator and may not have the correct degrees of freedom required to model the data. On the other hand, they allow the specification of sharp lateral changes in structure with relatively few unknown model parameters while an equivalent spherical harmonic expansion extends to very high harmonic degree. In practice, we perform calculations of synthetic seismograms by using the spherical harmonic basis because coupling between free oscillations of varying harmonic degree depends only upon some of the harmonic components of the model. Thus, models specified as a tectonic regionalization are first expanded in spherical harmonics.

One of the topics we consider in this paper is the qualitative effect of short wavelength structure on low-frequency data by computing synthetic seismograms for a tectonic regionalization expanded up to harmonic degree 40. The reason for our interest in such calculations is that the existing models leave much of the signal in the data unexplained. There are many possible reasons for this, e.g. approximate theories relating the data to the model have been used in the analyses and smooth models with only a few degrees of freedom have been sought. It is probable that some features of the data (e.g. surface wave amplitude anomalies) will require relatively short wavelength structure to model them and great care must be taken that any theoretical approximations will be adequate to the task. We are fortunate in low-frequency seismology that there are relatively complete algorithms for computing synthetic seismograms on an aspherical Earth (see, for example, Park & Gilbert 1986). Thus, given a model of three-dimensional structure, we are able to compute accurate synthetic seismograms for comparison with the data. This is still a computationally heavy task so an important aspect of such calculations is that they allow us to check approximate methods of seismogram calculation.

In the next section, we briefly consider the theoretical basis for the calculation of synthetic seismograms and show how differential seismograms can be constructed to allow fitting of complete waveforms or the spectra of small groups of modes. It is an observational fact that weakly coupled, split multiplets usually look like single resonance functions in the frequency domain so we consider an approximate theory which allows us to model the apparent centre frequencies and attenuation rates of such modes. Following sections discuss the ability of some current types of aspherical models to fit the observations and we make an attempt to catalogue those features of the Earth's aspherical structure which appear to have been robustly determined from low-frequency data.

Theoretical background

Low-frequency seismic data are most naturally analysed in the frequency domain and it is convenient to first consider the effect of aspherical structure on *isolated* multiplets. In reality, it is probably true that no multiplet can truly be regarded as isolated though coupling between multiplets is usually weak and most of the anomalous signal due to aspherical structure is caused by the interaction of singlets within a single multiplet. Coupling between multiplets causes small but measurable additional signals. First, consider the seismogram on a *spherical* Earth:

$$s(\boldsymbol{r}, t) = \sum_k \sum_{m=-l}^{l} \boldsymbol{\sigma}_k^m(\boldsymbol{r})\, a_k^m(\boldsymbol{r}_0)\, \mathrm{e}^{\mathrm{i}\omega_k t}, \tag{1}$$

where the real part is understood, $\boldsymbol{\sigma}_k^m$ are the $2l+1$ singlet eigenfunctions of the kth multiplet given by

$$\boldsymbol{\sigma}_k^m(\boldsymbol{r}) = \hat{\boldsymbol{r}} U_k(r)\, Y_l^m(\theta, \phi) + V_k(r) \nabla_1 Y_l^m(\theta, \phi) - W_k(r) \hat{\boldsymbol{r}} \times \nabla_1 Y_l^m(\theta, \phi), \tag{2}$$

PHILOSOPHICAL TRANSACTIONS OF THE ROYAL SOCIETY A MATHEMATICAL, PHYSICAL & ENGINEERING SCIENCES

where $\nabla_1 = \hat{\boldsymbol{\theta}}\partial_\theta + \operatorname{cosec}(\theta)\,\hat{\boldsymbol{\phi}}\partial_\phi$. For a point source at $\boldsymbol{r}_0$ with moment rate tensor M, the excitation coefficients, a_k^m, are given by $a_k^m = M : \epsilon_k^{m*}(\boldsymbol{r}_0)$, where ϵ_k^{m*} is the complex conjugate of the strain tensor of the mth singlet (Gilbert & Dziewonski 1975); ω_k is the degenerate frequency of the multiplet.

For notational convenience, we can consider $\boldsymbol{\sigma}_k^m$ and a_k^m to be arrays $2l+1$ in length so that the sum over m in (1) can be rewritten as a dot product. No confusion as to the vector nature of $\boldsymbol{\sigma}$ will arise if we consider only a single component of recording, i.e.

$$s(\boldsymbol{r}, t) = \sum_k \boldsymbol{\sigma}_k(\boldsymbol{r}) \cdot \boldsymbol{a}_k(\boldsymbol{r}_0)\, \mathrm{e}^{\mathrm{i}\omega_k t}. \tag{3}$$

The singlet eigenfunctions satisfy a variational principle, which we write schematically as

$$0 = L = V_0(\boldsymbol{\sigma}_i^*, \boldsymbol{\sigma}_j) - \omega_k^2\, T_0(\boldsymbol{\sigma}_i^*, \boldsymbol{\sigma}_j), \tag{4}$$

with $\delta L = 0$. V_0 is related to the potential energy and $\omega_k^2 T_0$ is related to the kinetic energy. T_0 is given by

$$T_0 = \int_V \rho_0\, \boldsymbol{\sigma}_i^* \cdot \boldsymbol{\sigma}_j \,\mathrm{d}V, \tag{5}$$

where ρ_0 is the density in the spherically averaged model. The eigenfunctions are orthogonal and are usually normalized so that

$$T_{0ij} = \delta_{ij}. \tag{6}$$

In the presence of rotation and small perturbations in structure, the symmetry of the original model is destroyed and the degeneracy is removed. Each of the $2l+1$ singlets in equation (1) now has a slightly different frequency. The variational principle now reads:

$$0 = L = V(\boldsymbol{s}^*, \boldsymbol{s}) + \omega W(\boldsymbol{s}^*, \boldsymbol{s}) - \omega^2 T(\boldsymbol{s}^*, \boldsymbol{s}), \tag{7}$$

with $\delta L = 0$. W is the Coriolis force interaction functional and V and T are the potential energy and kinetic energy interaction functionals (explicit expressions for these functionals can be found in Part & Gilbert 1986). We now expand $\boldsymbol{s}$ as a linear combination of spherical Earth singlets so that the new singlets are given by

$$\boldsymbol{s}_j = \sum_m U_{mj}\, \boldsymbol{\sigma}_k^m. \tag{8}$$

Substitution into (7) leads to a quadratic eigenvalue problem, but it is usually sufficiently accurate to replace ω in the Coriolis term with an average frequency, ω_k, say, so that equation (7) reduces to an ordinary eigenvalue problem (Park & Gilbert 1986). With the normalization given above, we have

$$V(\boldsymbol{\sigma}_i, \boldsymbol{\sigma}_j) = V_{ij} = \omega_k^2\, \delta_{ij} + \delta V_{ij},$$

$$T(\boldsymbol{\sigma}_i, \boldsymbol{\sigma}_j) = T_{ij} = \delta_{ij} + \delta T_{ij},$$

and can then define the *splitting matrix* $\boldsymbol{H}$

$$2\omega_k \boldsymbol{H} = \delta \boldsymbol{V} + \omega_k \boldsymbol{W} - \omega_k^2\, \delta \boldsymbol{T}. \tag{9}$$

With these definitions, we end up solving the following eigenvalue problem for the kth multiplet:

$$\boldsymbol{H}\boldsymbol{U} = \boldsymbol{U}\boldsymbol{\Omega}, \tag{10}$$

where $\omega_k + \Omega_{jj}$ are the new singlet frequencies and the eigenfunctions of $\boldsymbol{H}$ allow us to construct the new singlet eigenfunctions by using equation (8). The elements of the splitting matrix are given by (Woodhouse & Dahlen 1978)

$$H_{mm'} = \omega_k(a_k + mb_k + m^2 c_k)\,\delta_{mm'} + \sum_{s=2}^{2l} \gamma_s^{mm'}\, c_s^{m-m'}. \tag{11}$$

The first term gives the contribution of rotation and hydrostatic ellipticity of figure while the second gives the contribution of all other structure as specified by its spherical harmonic expansion, i.e. we let

$$\delta \boldsymbol{m}(\boldsymbol{r}) = \sum_{s,t} \delta \boldsymbol{m}_s^t(r)\, Y_s^t(\theta, \phi), \tag{12}$$

where

$$\delta \boldsymbol{m}_s^t(r) = (\delta\rho_s^t(r), \delta\kappa_s^t(r), \delta\mu_s^t(r), h_{sj}^t, \ldots), \tag{13}$$

with ρ being density, κ bulk modulus, h_j the radius of the jth discontinuity, etc. Then c_s^t is a linear functional of the s, t coefficient of each model parameter i.e.

$$c_s^t = \int_0^a \delta \boldsymbol{m}_s^t(r) \cdot \boldsymbol{G}_s(r)\, r^2\, \mathrm{d}r \tag{14}$$

and expressions for the kernels, $\boldsymbol{G}$, can be found in Woodhouse & Dahlen (1978). Finally, note that $\gamma_s^{mm'}$ can be written in terms of Wigner $3j$ symbols which can be computed using the recurrence relations given by Schulten & Gordon (1975). The $3j$ symbols are zero unless certain *selection rules* are satisfied. For an isolated multiplet, there is no contribution to (11) unless $0 \leqslant s \leqslant 2l$, s is even and $t = m - m'$.

The main point that we wish to emphasize is that the effect of aspherical structure on a particular multiplet is completely specified by the c_s^t which henceforth we shall call *structure coefficients*. Of course, we cannot directly determine the splitting matrix (and hence the structure coefficients) from the data because the seismogram is a nonlinear function of the splitting matrix. To see this, we use the eigenvalue–eigenvector decomposition of $\boldsymbol{H}$ given by equation (10) so that the aspherical Earth equivalent of equation (3) is

$$s(\boldsymbol{r}, t) = \sum_k (\boldsymbol{\sigma}_k\, \boldsymbol{U}_k)\, \mathrm{e}^{\mathrm{i}(\boldsymbol{\Omega}_k + \omega_k)t}\, (\boldsymbol{U}_k^{-1}\, \boldsymbol{a}_k). \tag{15}$$

This equation shows how each singlet on the aspherical Earth is, in general, a linear combination of all the singlets of the spherical Earth. An interesting exception arises if the multiplet is dominantly sensitive to axisymmetric structure. Such structure contributes only to the diagonal elements of $\boldsymbol{H}_k$ so $\boldsymbol{U}_k$ is, in this case, the unit matrix and there is no mixing of the spherical Earth singlets.

Equation (15) can be written in several ways which make the effect of aspherical structure clearer (Woodhouse & Girnius 1982). For example, we can regard $\boldsymbol{a}_k$ as being a slowly varying function of time which satisfies the equation:

$$\mathrm{d}\boldsymbol{a}_k/\mathrm{d}t = \mathrm{i}\boldsymbol{H}_k\, \boldsymbol{a}_k(t), \tag{16}$$

with the initial condition that at $t = 0$, $\boldsymbol{a}_k$ is defined as in equation (1). Then

$$s(\boldsymbol{r}, t) = \sum_k \boldsymbol{\sigma}_k(\boldsymbol{r}) \cdot \boldsymbol{a}_k(\boldsymbol{r}_0, t)\, \mathrm{e}^{\mathrm{i}\omega_k t}. \tag{17}$$

Equation (16) has the solution

$$\boldsymbol{a}_k(t) = \boldsymbol{P}_k(t)\, \boldsymbol{a}_k(0), \tag{18}$$

where $\boldsymbol{P}_k(t) = \exp(\mathrm{i}\boldsymbol{H}_k t)$ is the matrizant or propagator matrix; $\boldsymbol{a}_k$ can be thought of as an envelope function which varies on a long timescale because the magnitude of the splitting matrix is of the same order as the splitting width of the multiplet. Note that aspherical structure only appears in equation (17) through the time-dependence of $\boldsymbol{a}_k$.

We can extend this representation to compute differential seismograms so that the effect of perturbing a structure coefficient on the time series can be calculated. To do this, we differentiate equation (17) with respect to one of the c_s^t giving

$$\frac{\partial s}{\partial c_s^t} = \sum_k \boldsymbol{\sigma}_k \cdot \frac{\partial \boldsymbol{a}_k}{\partial c_s^t} \mathrm{e}^{\mathrm{i}\omega_k t}, \tag{19}$$

where $\partial \boldsymbol{a}_k / \partial c_s^t$ can be evaluated by differentiating equation (16) with respect to the c_s^t so yielding an inhomogeneous propagator equation whose solution is well known (Gilbert & Backus 1966; Ritzwoller *et al.* 1986). The differential seismograms may now be used to iteratively improve a set of structure coefficients so that equation (17) gives a good representation of the data (Woodhouse & Giardini 1985; Ritzwoller *et al.* 1986, 1988).

Before we leave the case of an isolated multiplet, we recast equation (17) into yet another form which is useful in developing an approximate theory to describe the spectra of unresolvably split multiplets. If we define a time dependent *location parameter* for the kth multiplet as

$$\lambda(t) = \boldsymbol{\sigma} \cdot \boldsymbol{H} \cdot \boldsymbol{a}(t) / \boldsymbol{\sigma} \cdot \boldsymbol{a}(t), \tag{20}$$

then equation (17) can be written

$$s(\boldsymbol{r}, t) = (\boldsymbol{\sigma} \cdot \boldsymbol{a}(0)) \exp\left(\mathrm{i} \int_0^t \lambda(t)\, \mathrm{d}t\right) \exp(\mathrm{i}\omega_k t). \tag{21}$$

If $\lambda(t)$ is only weakly dependent upon time, i.e. $\lambda(t) \approx \lambda(0) = \lambda_0$ say, then equation (21) reduces to

$$s(\boldsymbol{r}, t) = (\boldsymbol{\sigma} \cdot \boldsymbol{a}(0)) \exp(\mathrm{i}(\omega_k + \lambda_0) t), \tag{22}$$

which corresponds to a peak shift in the spectrum. This is the asymptotic result of Jordan (1978) and Dahlen (1979), which is valid in the limit that the wavelength of the structure is much longer than the wavelength of the mode (i.e. $s \ll l$). This result appears to be roughly valid for surface-wave equivalent modes with harmonic degree greater than about 20 for model M84A of Woodhouse & Dziewonski (1984). Figure 1 shows the actual time variation of $\lambda(t)$ for some modes and we do a much better job of modelling the data if we replace λ_0 in equation (23) with a time-average of the true $\lambda(t)$. Smith & Masters (1989) show how suitable time averages can be constructed which give a *complex* peak shift so modifying the apparent attenuation rate as well as the centre frequency of an unresolvably split multiplet. This theory works well with synthetic data constructed using M84A as the test model, but does not do a very good job of explaining observed peak shifts. Two possible reasons suggest themselves: (1) the Earth has significant power in structure of higher harmonic degree than is present in M84A and (2) coupling between multiplets significantly affects the observed peak shifts. This latter hypothesis can be tested by computing coupled mode synthetic seismograms.

Coupling between multiplets can be accommodated by returning to equation (7) and expanding $\boldsymbol{s}$ in the singlets of all the coupling multiplets. Much of the theory described above can be extended to the coupled multiplet case in an obvious way. Even equation (21) can be extended to the weakly coupled case because the singlets of weakly coupled multiplets clump into groups forming *hybrid* multiplets. Each singlet of the hybrid multiplet is a linear

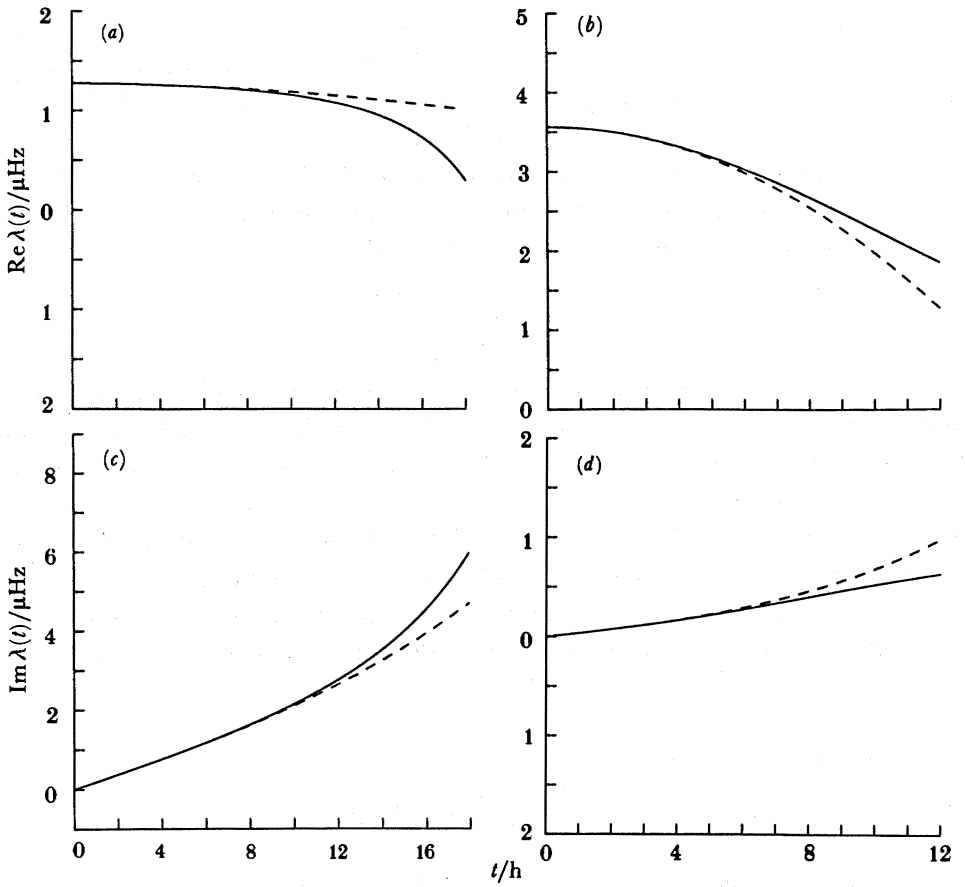

FIGURE 1. The generalized location parameter $\lambda(t)$ as a function of time. (*a*) and (*c*) show the real and imaginary parts of $\lambda(t)$ for ${}_0S_{24}$. (*b*) and (*d*) are the same but for ${}_0S_{36}$. The receiver was located in Guam for a source in Tonga. Model M84A with rotation was used to perform the calculation. Figure from Smith & Masters (1989).

combination of all the singlets of the coupling multiplets and it is possible to find the coefficients in this combination to first order in the coupling strength without performing a complete matrix decomposition (Park 1987; Dahlen 1987). Park calls this the *subspace projection method* and it may be used to define a location parameter for a hybrid multiplet. The selection rules for coupling between different multiplets can get quite complicated. The most obvious kind of coupling seen in the data is Coriolis coupling of ${}_nS_l$ modes to ${}_nT_{l\pm1}$ and in fact, significant coupling of fundamental spheroidal modes to fundamental toroidal modes occurs throughout the frequency band $1.5 \rightarrow 3$ mHz (Masters *et al.* 1983). Of course, this kind of coupling does not directly tell us about aspherical structure so of more interest is the fact that coupling of ${}_nS_l$ to its neighbours, ${}_nS_{l-1}$, ${}_nS_{l+1}$, etc., sensitizes the seismogram to structure of odd harmonic degree. We shall show some calculations which illustrate this effect later in the paper and an asymptotic treatment can be found in Park (1987) and Romanowicz (1987).

In the next sections we discuss some of the observations and the ability of available models to fit them. A more complete discussion of the low-frequency data can be found in Masters & Ritzwoller (1988). It is convenient to divide the observations into two categories; (1) large harmonic degree surface-wave equivalent modes which are dominantly sensitive to the structure of the upper mantle and (2) low harmonic degree, high Q modes which are also sensitive to the structure of the deep Earth.

PHILOSOPHICAL TRANSACTIONS OF THE ROYAL SOCIETY A MATHEMATICAL, PHYSICAL & ENGINEERING SCIENCES

Surface-wave modes and upper mantle models

The surface-wave equivalent modes are unresolvably split and may be amenable to interpretation by using asymptotic theory (assuming that the spectrum of aspherical structure is very red). The main approximation that is invoked in the asymptotic theory is that the data are sensitive to structure only along the great-circle path joining source and receiver. This approximation is theoretically justified for the mode peak shift data in the limit that $l \to \infty$ when equation (20) becomes

$$\lambda(t) = \lambda(0) = \sum_{s\,(\text{even})} P_s(0) \sum_t c_s^t Y_s^t(\Theta, \Phi), \tag{23}$$

where Θ, Φ is the location of the pole of the great circle joining the source and receiver (Jordan 1978). Centre frequencies and apparent attenuation rates are easy to measure for the highly excited fundamental spheroidal modes (figure 2) and, if one plots the observed peak shifts as symbols at the pole locations, one obtains maps such as in figure 3. A large-scale structure is

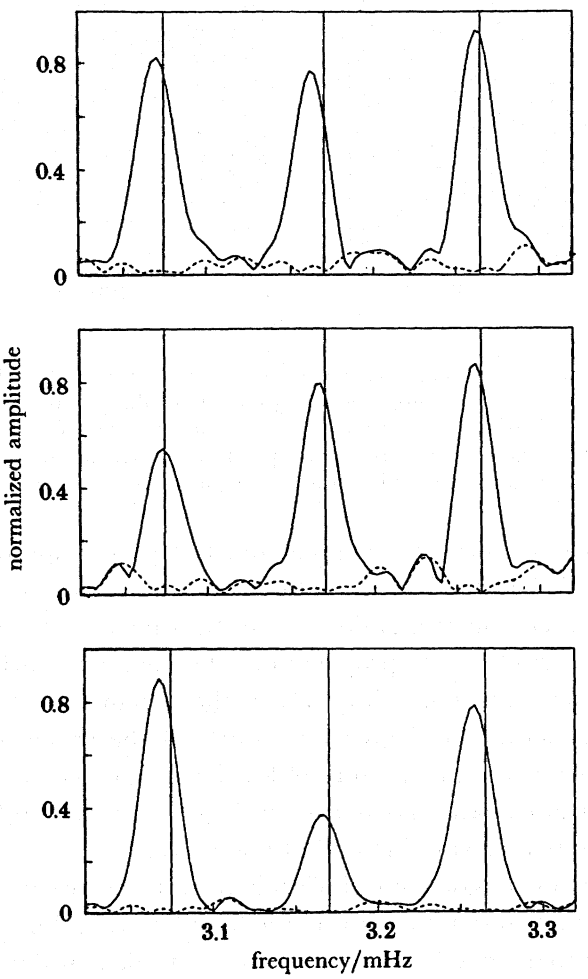

Figure 2. Linear amplitude spectra of a frequency band encompassing the modes ${}_0S_{22}$ to ${}_0S_{24}$. The solid line is the original spectrum while the dashed line is the residual after the best fitting resonance function has been removed from the data. Note that the resonance function model does a good job of modelling the data and that the apparent centre frequency of the modes is variable from record to record.

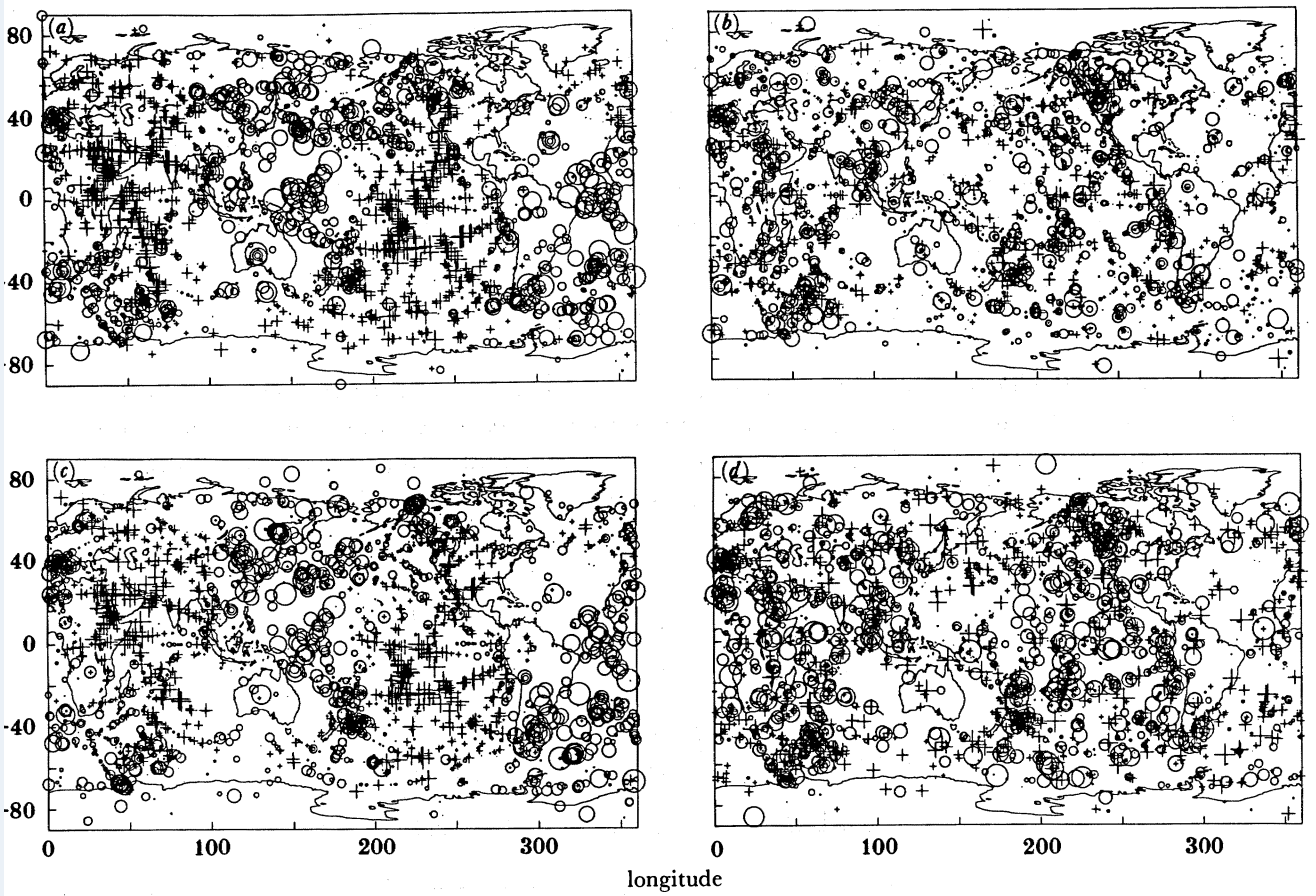

FIGURE 3. Frequency and attenuation perturbations for two modes plotted at the pole of the great-circle joining the source and receiver. The symbol size is proportional to the size of the perturbation. (*a*) and (*b*) show the frequency and attenuation perturbations respectively for ${}_0S_{22}$ and (*c*) and (*d*) are equivalent plots for ${}_0S_{42}$. Figure from Smith & Masters (1989). Open circles correspond to negative perturbations and pluses to positive perturbations. The largest symbols correspond to a 0.4% frequency perturbation.

apparent in the real part frequency observations, but the attenuation observations show no such pattern. The peak shift data can be inverted to retrieve structure coefficients (figure 4) by using either the asymptotic relation of equation (23) or by using a more complete theory which takes account of off-great-circle path propagation. Tremendous variance reductions are possible using the frequency shift data with most of the variance in the observations being explained by a pattern of harmonic degree two. Little of the variance in the attenuation measurements can be explained with structure of low harmonic degree. The frequency shifts also seem to robustly constrain a pattern of harmonic degree six (Davis 1987; Smith & Masters 1989), but other structure is very variable and of low power.

A gross test of the reasonableness of a model of aspherical structure can be had by comparing the theoretical splitting widths of multiplets (i.e. the frequency band occupied by the singlets of the multiplet) with the frequency band covered by the peak shift data (figure 5). We find that a model like M84A tends to underpredict the splitting widths of fundamental spheroidal modes but that a tectonic regionalization (see below) with a little more power in the lower

PHILOSOPHICAL TRANSACTIONS OF THE ROYAL SOCIETY A MATHEMATICAL, PHYSICAL & ENGINEERING SCIENCES

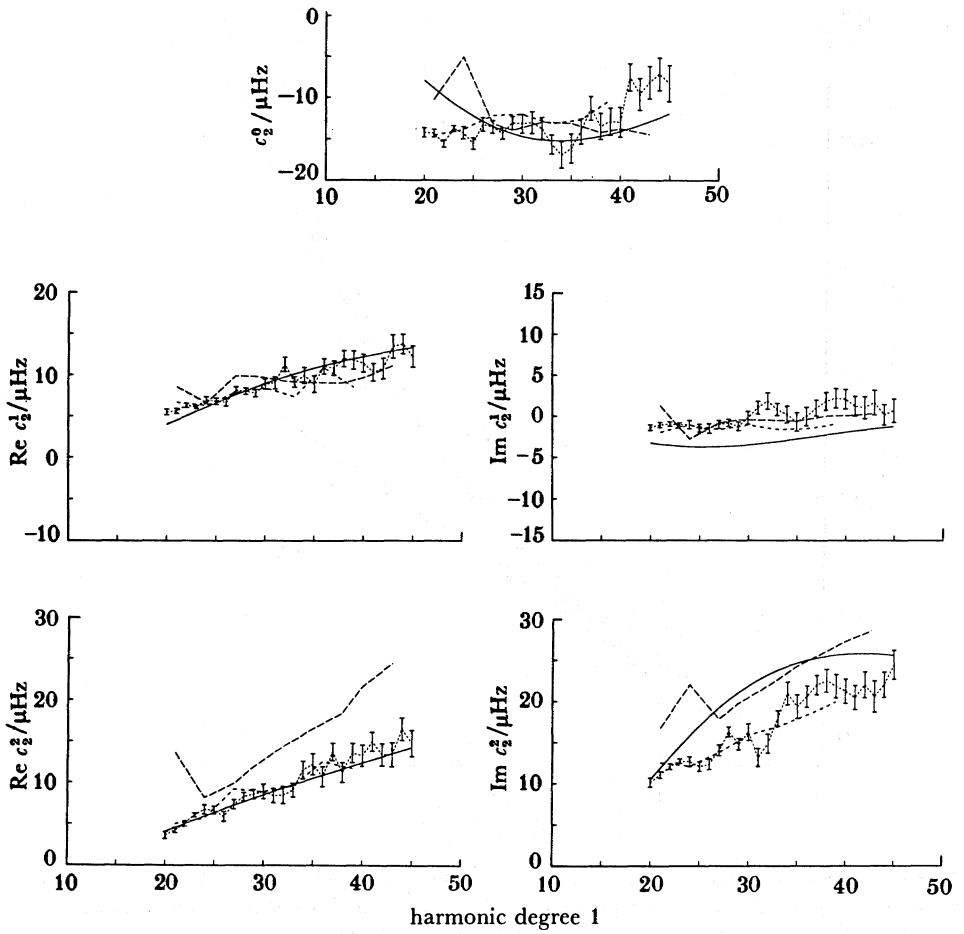

FIGURE 4. Structure coefficients, c_2^t for the fundamental spheroidal modes showing the coefficients of Smith & Masters (1989) (data with error bars) compared with the predictions of M84A (solid line), the results of Davis (1987) (intermediate dashed line), and the results of Nakanishi & Anderson (1983) (long dashed line). Agreement is quite good for these coefficients, but is worse at higher harmonic degrees. Figure from Smith & Masters (1989).

harmonic degrees is capable of giving a qualitative fit. Note that the regionalization including harmonics up to degree 40 gives almost identical results to the regionalization truncated at harmonic degree 10 so there is no *a priori* reason why models with sharp edges cannot give a good fit to the data.

Of course, one need not confine oneself to the interpretation of peak shift data and both waveform fitting techniques (Woodhouse & Dziewonski 1984; Tanimoto 1987) and surface wave dispersion measurements (Nakanishi & Anderson 1983, 1984) have been used. All interpretations have assumed that off-path propagation can be ignored. The waveform fitting experiment of Woodhouse & Dziewonski deserves further comment as these authors do not try to constrain the structure coefficients of individual multiplets, but directly invert for a parametrized form of $\delta m_s^t(r)$ (see equation (14)). The predictions of their model M84A of the structure coefficients of some fundamental modes are compared with the results of the peak

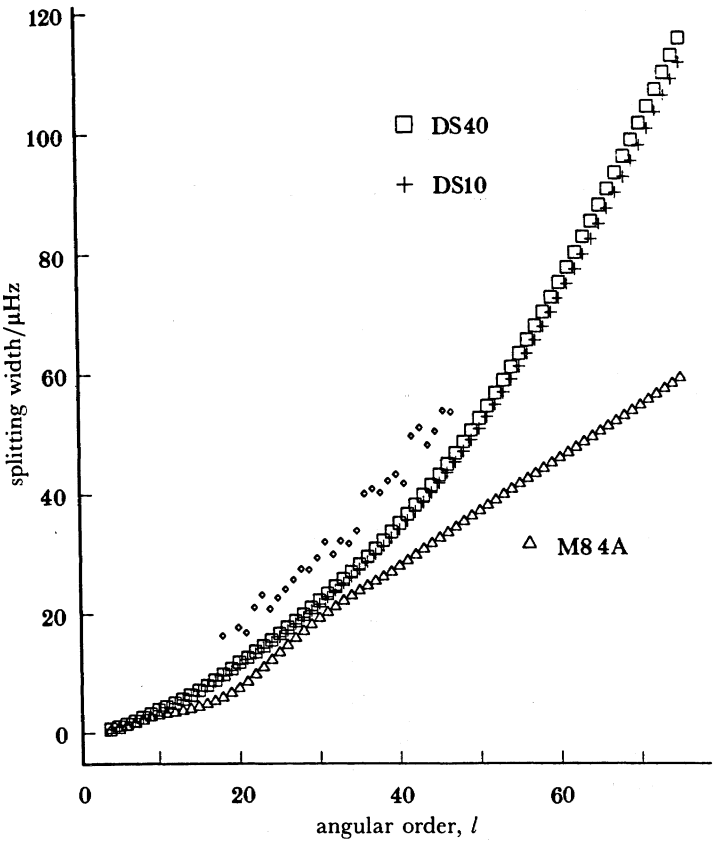

FIGURE 5. Splitting widths of fundamental spheroidal modes predicted by M84A (triangles), the tectonic regionalization of Dziewonski & Steim expanded in spherical harmonics and truncated at harmonic degree 40 (DS40) or harmonic degree 10 (DS10). The diamonds are the observations.

fitting experiment in figure 4. A convenient way of comparing different models is to plot the *splitting functions* (Woodhouse *et al.* 1986) defined by

$$\sum_{s,t} c_s^t \, Y_s^t(\theta, \phi). \tag{24}$$

We illustrate this in figure 6, where we see that agreement of the degree 2 pattern is quite good (as it should be as this accounts for over 60% of the variance in the data), but even the quite well-determined degree 6 structure shows significant differences. Numerical experiments indicate that the degree 6 structure is not reliably determined if the asymptotic theory (equation (23)) is used to interpret the peak shift data because the signal from non-asymptotic effects rivals that of the structure itself. Thus it may be true that the degree 6 structure in M84A is biased by the use of the great-circle approximation. As the power in harmonic degrees 4 and 8 is even smaller than that in degree 6, it is unsurprising that there is as yet little agreement as to the shapes of the splitting functions at these harmonic degrees. Comparisons with the surface-wave dispersion data show even less agreement which may reflect the difficulty of accurately determining phase velocity at very long periods.

Model M84A also includes structure of odd harmonic degree by using the difference in phase

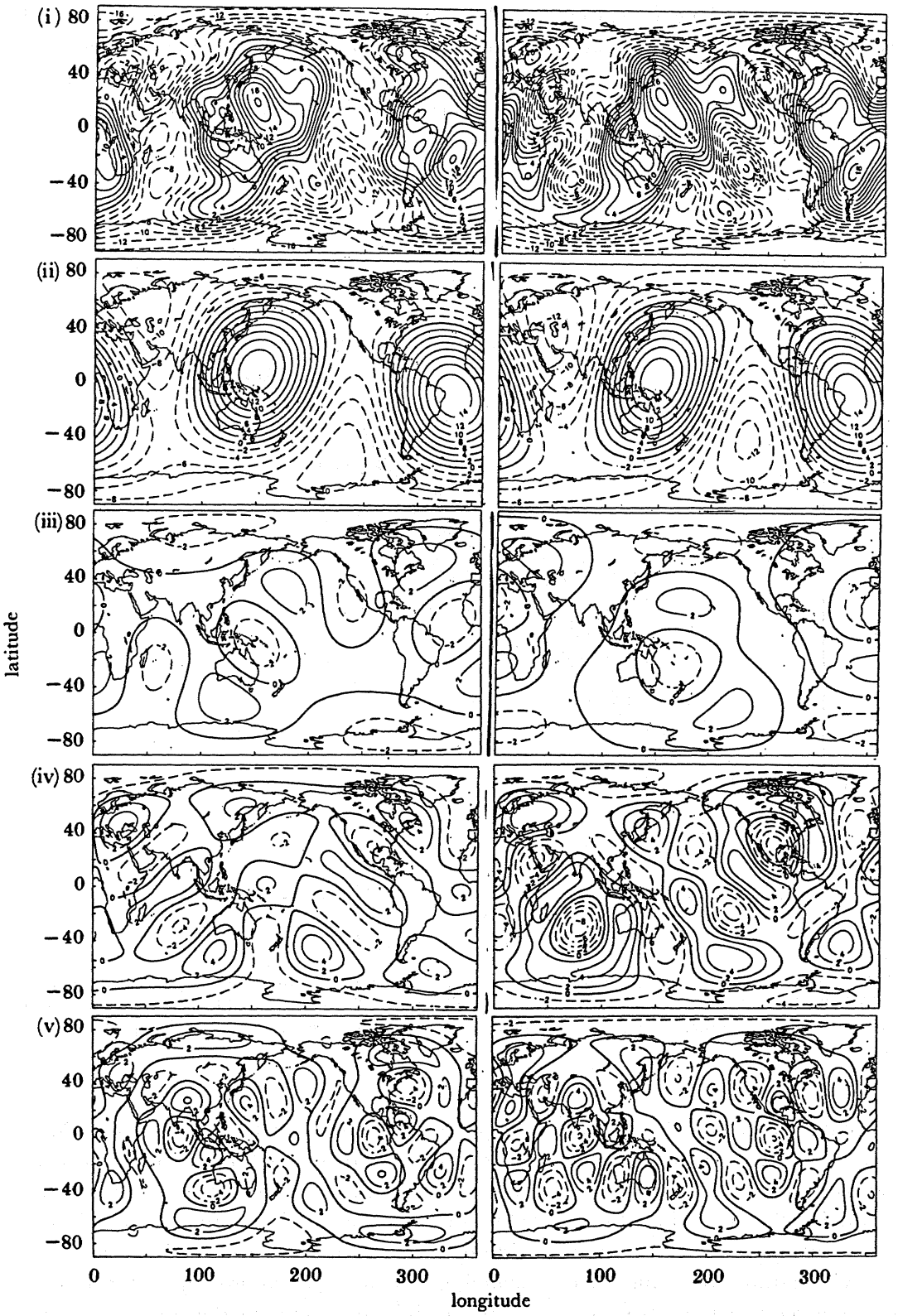

FIGURE 6. Contour plots of the splitting function of mode ${}_0S_{23}$ as determined from peak shift data (left column) and as predicted by M84A (right column); (i) degrees, 2–8, (ii) degree 2, (iii) degree 4, (iv) degree 6, (v) degree 8. Agreement is very good at degree 2 but deteriorates at higher harmonic degree. Note that degree 2 dominates the overall pattern. Figure from Smith & Masters (1989).

PHILOSOPHICAL TRANSACTIONS OF THE ROYAL SOCIETY A MATHEMATICAL, PHYSICAL & ENGINEERING SCIENCES

anomaly accumulated along a great-circle and the minor arc. This time domain signal may be the only way of seeing odd-order structure in low-frequency data because experiments with synthetic data show that peak shift measurements are little affected by odd-order structure of the magnitude present in the current models. Figure 7 shows a comparison of peak shift measurements made from synthetic seismograms for model DS40 with and without coupling

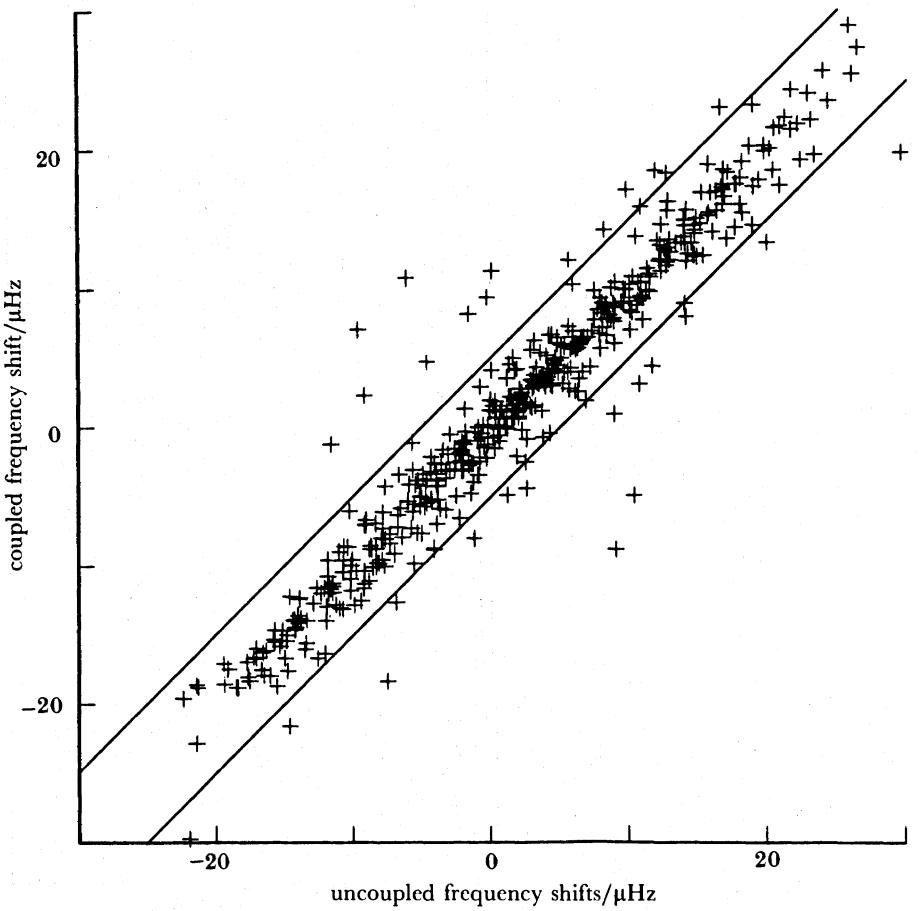

FIGURE 7. A comparison of centre frequency measurements of ${}_0S_{50}$ made from synthetic seismograms computed from model DS40 with and without along-branch coupling. The lines indicate the probable measurement error and it is clear that the odd-order structure in this model contributes a very small signal which is probably below the measurement error.

between neighbours along the fundamental spheroidal mode branch. The results for M84A show even less scatter and the only obvious discrepancies are for small peaks close to nodes in radiation patterns which would probably not be measured in practice. The next question that arises is whether the great-circle theory used to interpret the data in the time domain leads to errors that swamp the signal from the odd-order structure. To check this, we computed synthetic seismograms by using various coupling schemes and approximate theories and computed the relative root mean square (r.m.s.) difference between the first ten hours of recording and averaged the results over roughly 100 source-receiver pairs. We present the average results in matrix form in table 1. Seismograms constructed using the theory of

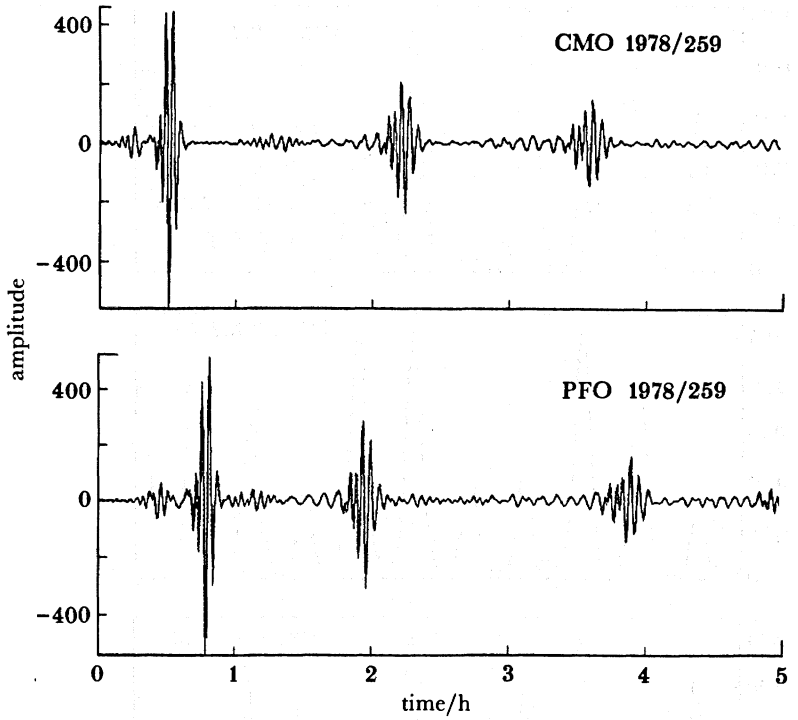

FIGURE 8. Comparisons of along-branch coupled mode synthetic seismograms (dashed line) with uncoupled mode synthetic seismograms (solid line). The case of CMO is typical while an extreme example is given by PFO. The calculations have been performed with M84A as the aspherical structure and include the first three branches up to a frequency of 8 mHz. The effect of coupling is so small that it is extremely difficult to distinguish the two calculations.

Woodhouse & Dziewonski do seem to fit the precise calculations slightly better than the calculations ignoring along-branch coupling (i.e. an r.m.s. difference of 13 % against 17 %). One thing that is noticeable from table 1 is that all the numbers are relatively small. An r.m.s. difference of about 15 % corresponds to an almost exact visual overlay of the time series (figures 8 and 9) and we would be well satisfied if we could fit the actual data to this precision. Needless

TABLE 1. MEAN RELATIVE R.M.S. RESIDUAL BETWEEN SEISMOGRAMS COMPUTED WITH DIFFERENT THEORETICAL SCHEMES

(The numbers are in percent and are the averages of the first 10 hours of 80 recordings. The aspherical model is M84A. 'Coupled-5' indicates a calculation where the singlets of five adjacent fundamental modes have been coupled together whereas 'coupled-3' implies a calculation with coupling to nearest neighbours. 'WD84' implies a calculation using a the theory of Woodhouse & Dziewonski (1984) while 'isolated' includes no mode coupling at all. 'Peak shift' implies a calculation with only the asymptotic shift in the peak frequencies and 'spherical' is the spherical Earth calculation. All fundamental spheroidal modes up to a frequency of 8 mHz have been included and the time series have been low-passed with a corner at 6.5 mHz to reduce the effect of ringing.)

	coupled-5	coupled-3	WD84	isolated	peak shift	spherical
coupled-5	0	9.8	13.0	18.3	19.6	30.5
coupled-3	—	0	13.6	17.0	18.3	29.6
WD84	—	—	0	20.7	18.7	31.1
isolated	—	—	—	0	5.9	22.0
peak shift	—	—	—	—	0	21.2
spherical	—	—	—	—	—	0

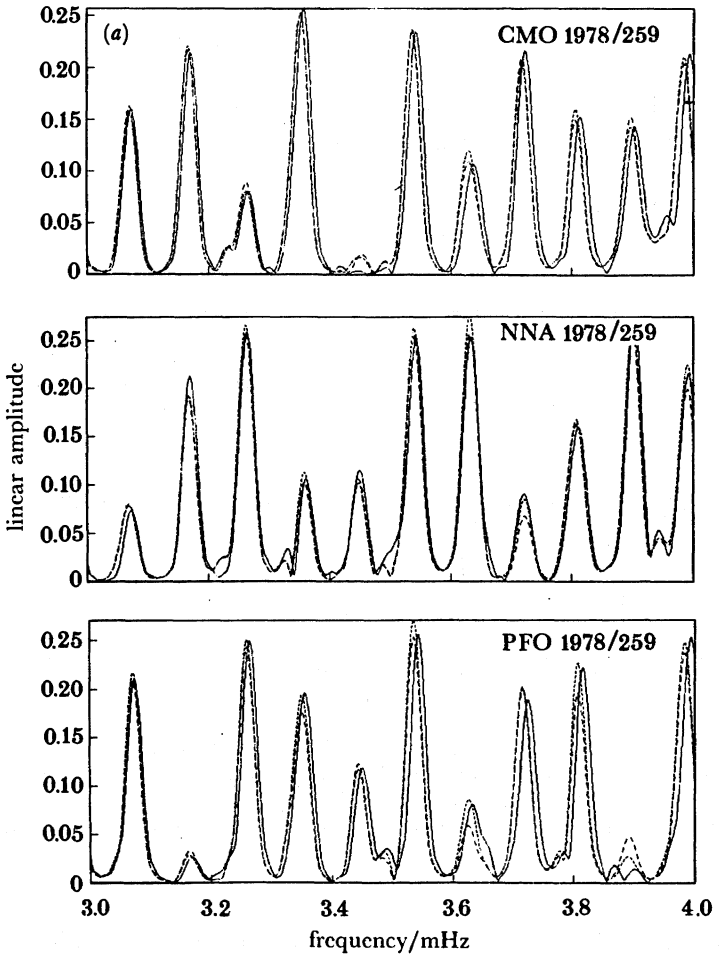

FIGURE 9a. For description see opposite.

to say, we do not do this well and it seems that M84A substantially underpredicts the magnitude of the variations in waveforms that we observe.

What is wrong with the model? There are several possibilities though experiments with synthetic seismograms suggest that the problem is probably not with elastic structure of low harmonic degree. In particular, enhancing the odd-order structure to increase the effect of along-branch coupling does not seem to help. Extreme lateral variations in the attenuation structure of the Earth may be a possibility or, more likely, the effect of higher order structure than that considered heretofore may be important. To investigate this latter possibility, we have expanded an example of a tectonic regionalization into spherical harmonics (Dziewonski & Steim 1982) and constructed a large suite of synthetic seismograms using various coupling schemes (this work was done in collaboration with Dr Ivan Henson). The regionalization, along with its spherical harmonic representation up to harmonic degree 40 is shown in figure 10. Because such models have sharp edges, the power in each harmonic degree falls off quite slowly (figure 11).

The relative r.m.s. residuals between the first ten hours of seismograms computed using different recipes are shown in table 2. Note that the numbers are roughly double those for

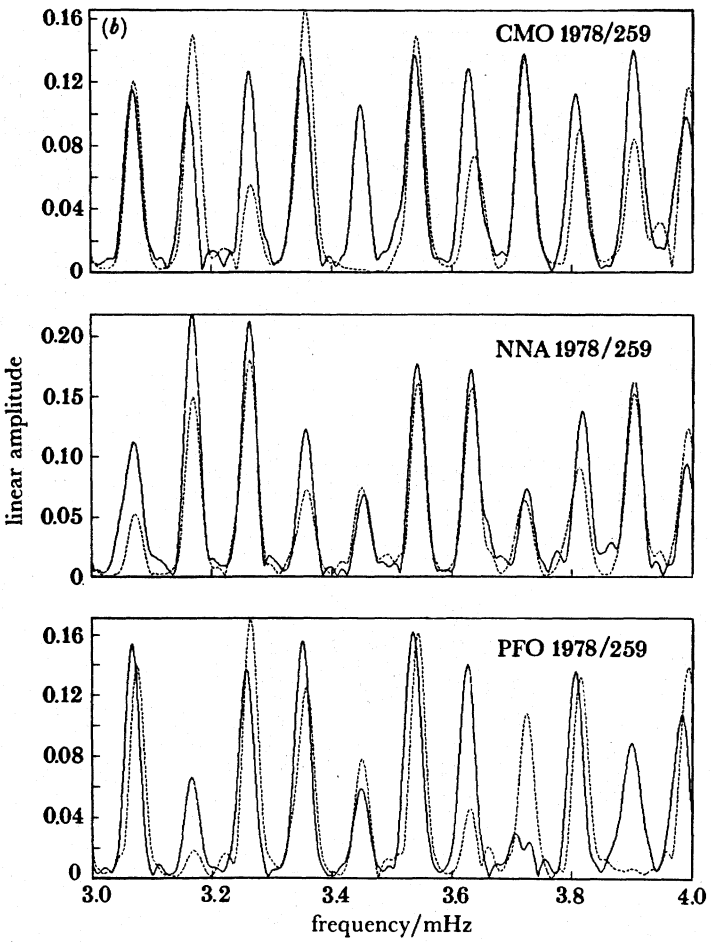

FIGURE 9. (*a*) Theoretical amplitude spectra of 20 hours of the recordings described in figure 8. The solid line is for a spherical Earth, the short dashed line assumes multiplets are isolated and the long dashed line includes along-branch coupling. The main effect of the aspherical model is to cause peak shifting and small amplitude perturbations. (*b*) As in (*a*), but showing the real data (solid line) in lieu of the spherical Earth seismogram. Note the strong amplitude anomalies that are not present in the theoretical calculation.

M84A and are more similar to the data. Also note that seismograms constructed with the method of Woodhouse & Dziewonski are sometimes worse fits to the most complete calculations than seismograms computed without any coupling at all. The higher order structure in this model has little effect on peak frequency shifts, but figure 12 does show that the apparent attenuation measurements are now quite strongly affected by the structure. Again, this is similar to the behaviour we observe in the data.

In summary, while a model like DS40 does not provide a quantitative fit to the data (indeed it doesn't even predict the degree 2 pattern seen in the peak frequency data), the presence of relatively low power, high harmonic degree structure does seem to produce qualitatively similar signals to those in the data. The presence of such higher-order structure may cause approximate theoretical representations to give biased answers particularly in the odd-order structure whose effects are only weakly apparent in the data (see also Park 1986).

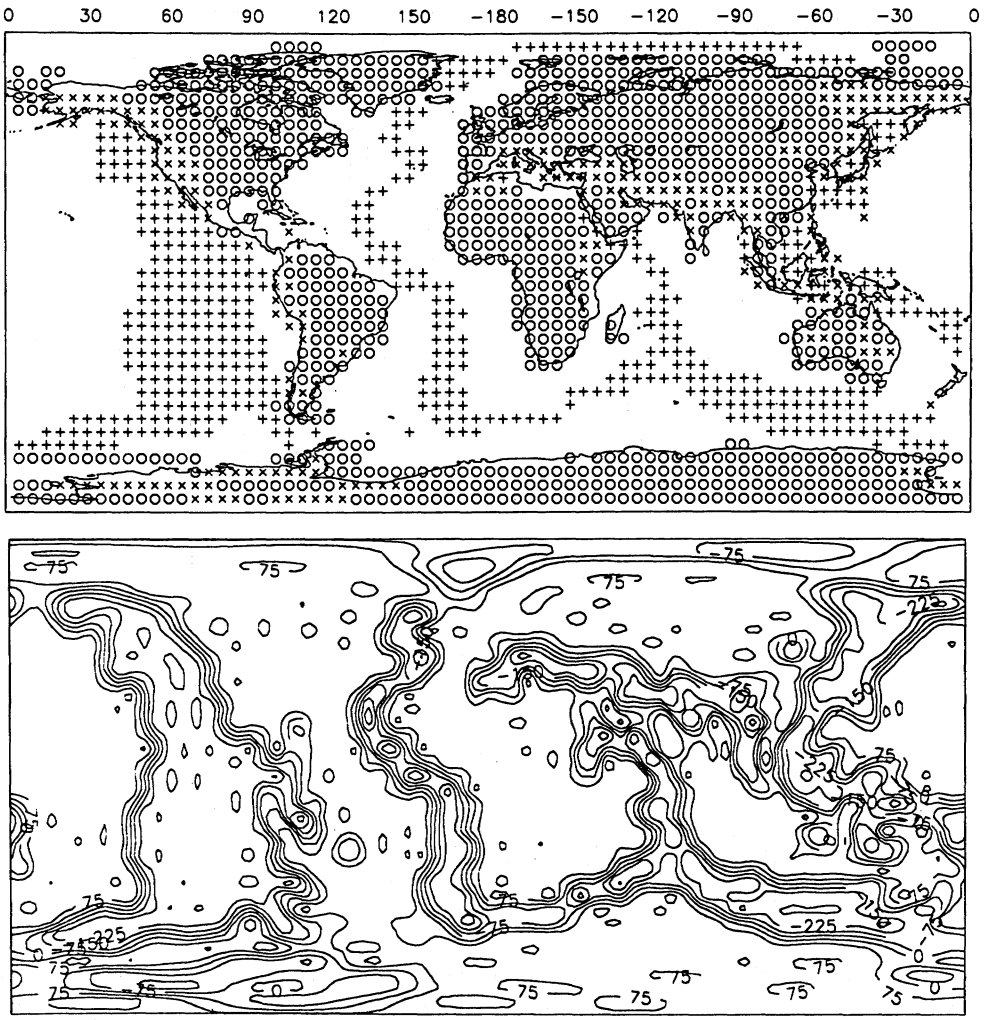

FIGURE 10. The tectonic regionalization of Dziewonski & Steim along with the expansion up to harmonic degree 40 of the lateral variation in shear velocity in one of the layers of this model.

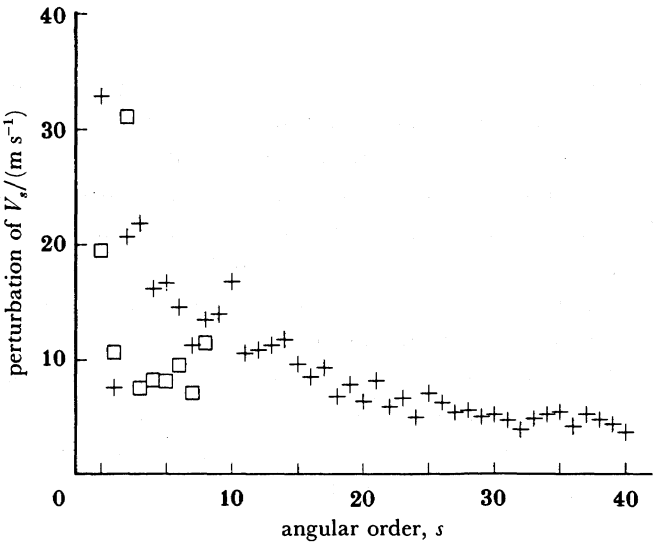

FIGURE 11. A comparison of the average amplitude in each harmonic degree of DS40 and M84A at a depth corresponding to the transition zone of the Earth. Note the dominant degree 2 part of M84A and the slow fall-off of the power in DS40.

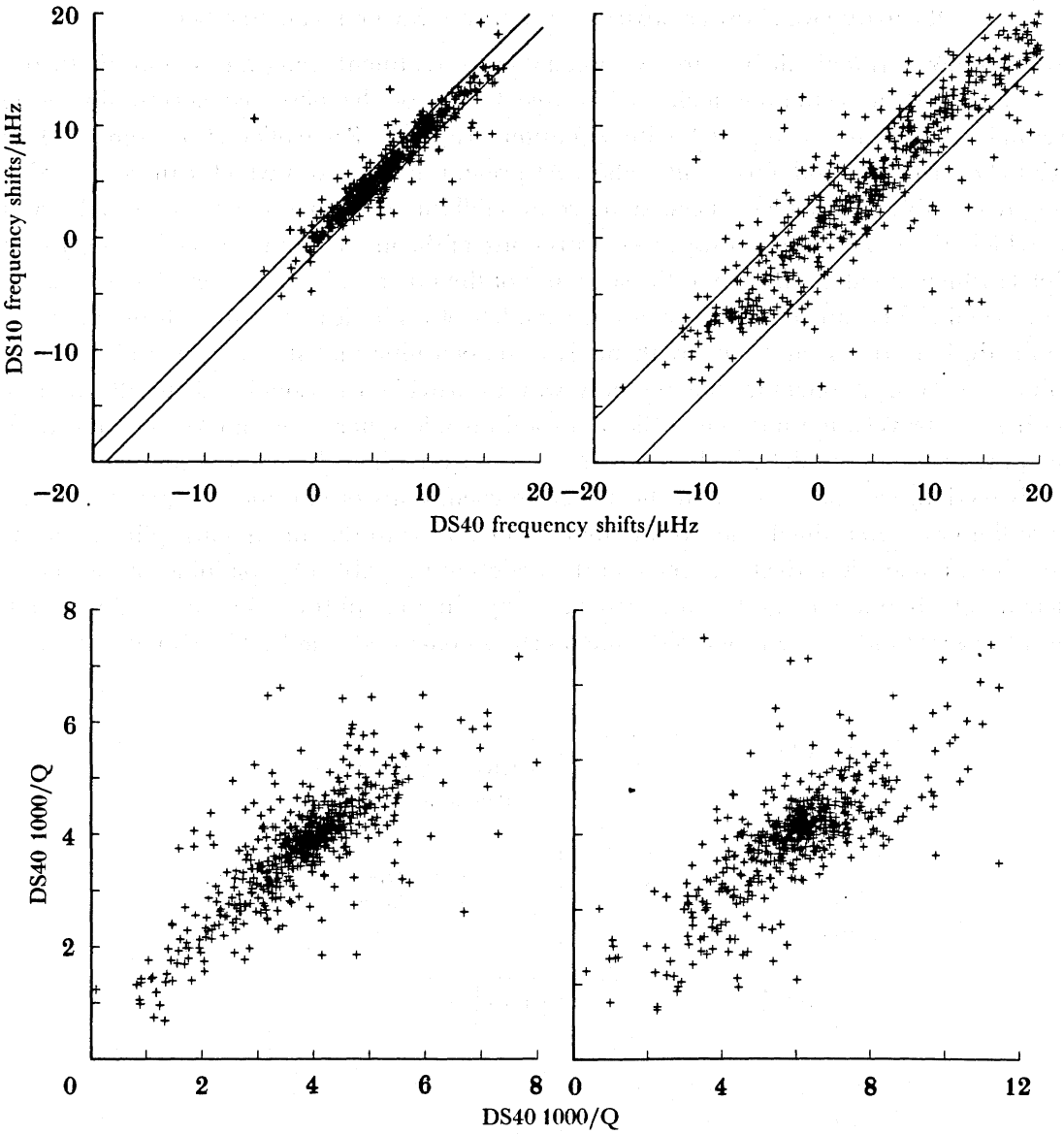

FIGURE 12. An illustration of the effect of higher-order structure on the centre frequencies and attenuation rates of ${}_0S_{23}$ (left column) and ${}_0S_{43}$ (right column). The scatter away from a straight line is solely due to structure of harmonic degree greater than 10. The centre frequencies show much less effect than the apparent attenuation implying that higher-order structure may cause some of our inability to model the attenuation data.

TABLE 2. AS FOR TABLE 1 BUT USING THE TECTONIC REGIONALIZATION

	coupled-5	coupled-3	WD84	isolated	peak shift	spherical
coupled-5	0	18.2	32.7	32.9	41.1	58.2
coupled-3	—	0	36.4	27.2	36.4	54.5
WD84	—	—	0	44.1	32.0	57.0
isolated	—	—	—	0	23.2	46.3
peak shift	—	—	—	—	0	43.4
spherical	—	—	—	—	—	0

Resolvably split modes and deep Earth structure

Modes of low harmonic degree are not amenable to treatment using an asymptotic theory and we must use a technique such as iterative fitting of the observed spectra by using differential seismograms computed with equation (19) (see Ritzwoller *et al.* 1986, 1988; Giardini *et al.* 1987; Woodhouse *et al.* 1986). At present, only modes which can be regarded as being reasonably isolated have been analysed and fall into two categories: (1) normally split modes which are dominantly sensitive to the structure of the mantle and (2) very strongly split multiplets which are also sensitive to the structure of the inner and outer cores. The estimated structure coefficients can be used to constrain models of aspherical structure throughout the whole Earth, but are not sufficient by themselves to determine that structure unambiguously. Giardini *et al.* (1987) conclude that the only way to provide a reasonable fit to all the data (including the travel time data) is to have an anisotropic inner core and Woodhouse *et al.* (1986) present such a model which goes part way to explaining the observations.

In this section, we concentrate on the structure coefficients of harmonic degree 2 because they are the best determined and are the main contributor to the anomalous splitting of the core-sensitive modes. Relatively simple mantle models are capable of explaining the structure coefficients of all but ten modes and can also explain the splitting functions of the high harmonic degree fundamental spheroidal modes (Ritzwoller *et al.* 1988). These models are also

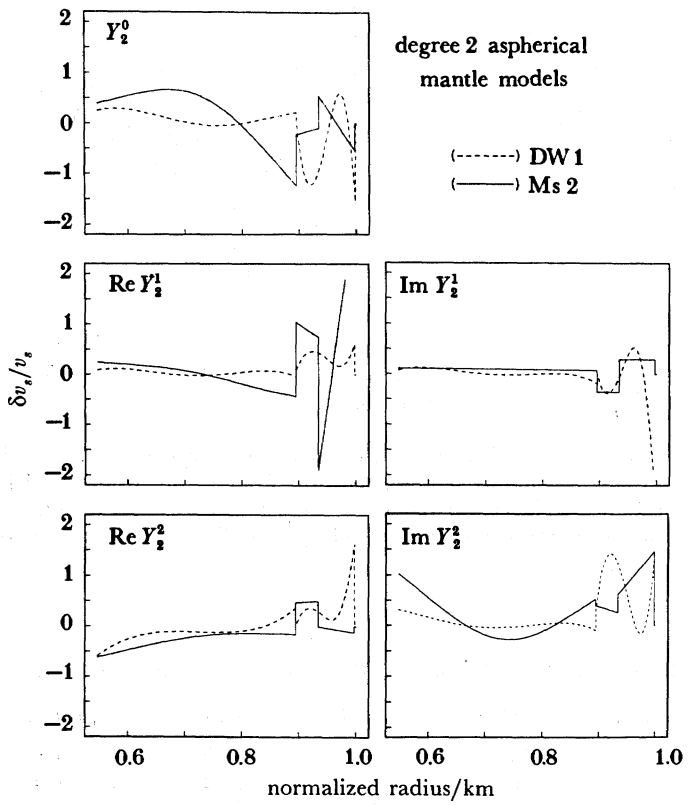

Figure 13. A degree 2 mantle model expressed as a relative perturbation in shear velocity derived from structure coefficients (solid line-Ms2) compared with a model which is a union of the upper mantle and lower mantle models of Dziewonski & Woodhouse (dashed line-DW1). Figure from Ritzwoller *et al.* (1988).

quite similar to the models derived from travel-time data (see, for example, Dziewonski 1984) except near the top of the lower mantle where the travel-time models have low sensitivity. The radial dependence of the harmonic degree 2 perturbations in shear velocity for one such model are shown in figure 13 and compared with a combination of models from the Harvard group. There are discrepancies in the upper mantle, but trade-offs with structure on internal discontinuities mean that it is difficult to construct a well-constrained model in this region. These models do not explain the structure coefficients of the ten anomalous core-sensitive modes. The most anomalous structure coefficient for those modes is c_2^0 which can be partially fit by introducing various kinds of anomalous structure into the core. It should be emphasized that the splitting of these modes is not a small signal as they have splitting widths between two and three times greater than that predicted by a rotating Earth in hydrostatic equilibrium. Figure 14 demonstrates that our mantle models do not fit these data though the addition of

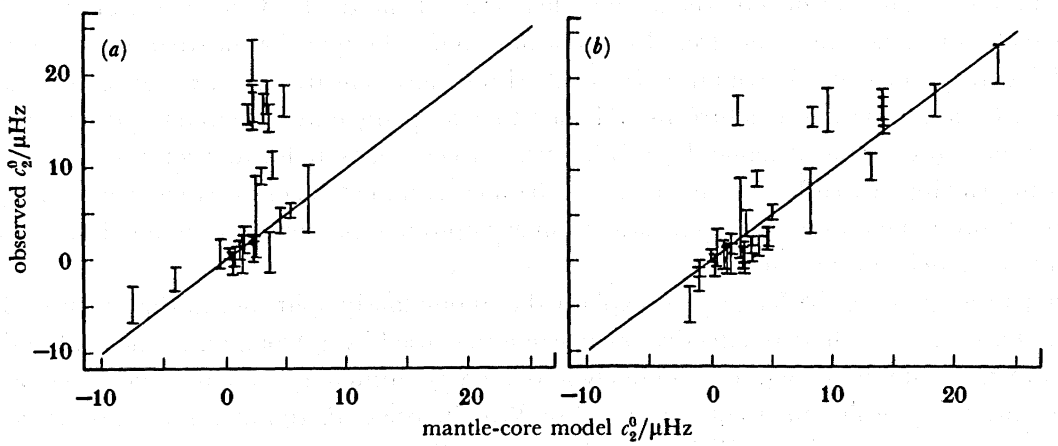

FIGURE 14. Observered c_2^0 coefficients plotted (*a*) against the predictions of the mantle model Ms2. (*b*) against the predictions of Ms2 which also includes some topography on the boundaries of the core and and isotropic heterogeneity in the inner core. Figure from Ritzwoller *et al.* (1988).

some topography on the boundaries of the outer core and a volumetric perturbation in the inner core go a long way to explaining the observations. The least well-fit modes are, unfortunately, the least well constrained by the observations so the poor fit to modes like ${}_3S_2$ may or may not be significant (Ritzwoller *et al.* 1988). While a model including anisotropy of the inner core can give a slightly better fit to some of the most anomalous modes (Woodhouse *et al.* 1986) it is likely that we will have to await an expansion of the data-set and an improvement in our knowledge of mantle structure before a definitive explanation for the splitting of these modes can be found.

CONCLUSIONS

The first round of modelling signals from aspherical structure in low-frequency data has produced some surprising results. In my opinion, the most surprising is that structure of harmonic degree 2 is dominant in the data and that the predictions of a rotating Earth in hydrostatic equilibrium are almost *never* fulfilled. This result is even more surprising when it is remembered that the surface of the Earth has a flattening that is very close to the theoretically

PHILOSOPHICAL TRANSACTIONS OF THE ROYAL SOCIETY A MATHEMATICAL, PHYSICAL & ENGINEERING SCIENCES

predicted value yet even a 300 second Rayleigh wave thinks that the Earth is round rather than elliptical. We seem to be able to produce models of large-scale structure in the mantle that go some way to explaining the largest-scale signals but the construction of synthetic seismograms for these models show that we have a long way to go. In fact, it is probably true that our best models predict seismograms which are closer to the predictions of a purely spherical Earth model than to the real data. We have yet to tie down the reason for this inability to mode the actual waveforms in detail but the answer probably lies in a rather unglamorous combination of higher-order structure and complicated coupling effects.

As far as the dominant signals in the seismogram are concerned (the surface-wave equivalent modes) most investigators agree on structure coefficients of harmonic degree 2 and (to a lesser extent) structure of harmonic degree 6, though a model of aspherical structure predicting these effects is by no means uniquely determined from these data. In particular, there are severe trade-offs between volumetric perturbations and structure on internal discontinuities in the upper mantle so that we do not yet have a clear idea of the depth dependence of even the largest-scale upper mantle structure. On top of this comes the question of whether or not we should 'correct' for crustal structure. It is surprising how sensitive even quite long-period surface waves are to crustal structure and it is easy to swamp any natural signal in the data with a correction that essentially demands an 'anti-crust' to compensate for it. Such questions are, at least in principle, capable of being answered by a careful analysis of overtone wave-packets though it is probable that we must get away from asymptotic representations of the data before a definitive model can be constructed.

Perhaps the greatest challenge is to explain the anomalously split modes that sample the core. Esoteric effects such as an effective shear strength caused by a strong magnetic field in the outer core can easily be shown to be unlikely and we may ultimately have to appeal to effects like the anisotropy in the inner core proposed by Woodhouse *et al.* 1986. It is also noteworthy that recent attempts at the modelling of the spherically averaged structure by using very accurate degenerate mode frequencies have met with difficulties when it comes to finding adequate models of the deepest Earth structure and there may be something fundamentally wrong with our conception of what this region of the Earth looks like (F. Gilbert, personal communication). It is also true that our modelling efforts are based upon the analysis of relatively few modes and an expansion of the data-set is required before emphatic statements about the structure of the deep Earth can be made.

I thank Mike Ritzwoller, Ivan Henson, Mark Smith and Rudolf Widmer for their invaluable contributions to this work, of course, all errors and omissions remain my responsibility alone. This research was supported by National Science Foundation grants EAR-84-10369 and EAR-84-18471. Most of the computations were performed on the Cray X-MP at the San Diego Supercomputer Center.

References

Dahlen, F. A. 1979 *Geophys. Jl R. astr. Soc.* **58**, 1–33.
Dahlen, F. A. 1987 *Geophys. Jl R. astr. Soc.* **91**, 241–254.
Davis, J. P. 1987 *Geophys. Jl R. astr. Soc.* **88**, 693–722.
Dziewonski, A. M. 1984 *J. geophys. Res.* **89**, 5929–5952.
Dziewonski, A. M. & Steim, J. 1982 *Geophys. Jl R. astr. Soc.* **70**, 503–527.
Giardini, D., Li, X.-D. & Woodhouse, J. H. 1987 *Nature, Lond.* **325**, 405–409.

PHILOSOPHICAL TRANSACTIONS OF THE ROYAL SOCIETY A MATHEMATICAL, PHYSICAL & ENGINEERING SCIENCES

Gilbert, F. & Backus, G. 1966 *Geophysics* **31**, 326–332.
Gilbert, F. & Dziewonski, A. M. 1975 *Phil. Trans. R. Soc. Lond.* A **278**, 187–269.
Jordan, T. H. 1978 *Geophys. Jl R. astr. Soc.* **52**, 441–455.
Masters, G., Park, J. & Gilbert, F. 1983 *J. geophys. Res.* **88**, 10285–10298.
Masters, G. & Ritzwoller, M. 1988 In *Mathematical geophysics*, pp. 1–30. Dordrecht: D. Reidel.
Nakanishi, I. & Anderson, D. L. 1983 *J. geophys. Res.* **88**, 10267–10283.
Nakanishi, I. & Anderson, D. L. 1984 *Geophys. Jl R. astr. Soc.* **78**, 573–618.
Park, J. 1986 *J. geophys. Res.* **91**, 6441–6464.
Park, J. 1987 *Geophys. Jl R. astr. Soc.* **90**, 129–169.
Park, J. & Gilbert, F. 1986 *J. geophys. Res.* **91**, 7241–7260.
Ritzwoller, M., Masters, G. & Gilbert, F. 1986 *J. geophys. Res.* **91**, 10203–10228.
Ritzwoller, M., Masters, G. & Gilbert, F. 1988 *J. geophys. Res.* **93**, 6369–6396.
Romanowicz, B. 1987 *Geophys. Jl R. astr. Soc.* **90**, 75–100.
Schulten, K. & Gordon, R. 1975 *J. math Phys.* **16**, 1961–1970.
Smith, M. F. & Masters, G. 1989 *J. geophys. Res.* **94**, 1953–1976.
Tanimoto, T. 1987 *Geophys. Jl R. astr. Soc.* **89**, 713–740.
Woodhouse, J. H. & Dahlen, F. A. 1978 *Geophys. Jl R. astr. Soc.* **53**, 335–354.
Woodhouse, J. H. & Dziewonski, A. M. 1984 *J. geophys. Res.* **89**, 5953–5986.
Woodhouse, J. H. & Girnius, T. P. 1982 *Geophys. Jl R. astr. Soc.* **68**, 653–673.
Woodhouse, J. H. & Giardini, D. 1985 *Eos, Wash.* **66**, 300.
Woodhouse, J. H., Giardini, D. & Li, X.-D. 1986 *Geophys. Res. Lett.* **13**, 1549–1552.

PHILOSOPHICAL TRANSACTIONS OF THE ROYAL SOCIETY A MATHEMATICAL, PHYSICAL & ENGINEERING SCIENCES